Isolation and characteristics of CD133$^-$/A2B5$^+$ and CD133$^-$/A2B5$^-$ cells from the SHG139s cell line

YONG HAN*, HANGZHOU WANG*, YULUN HUANG, ZHE CHENG, TING SUN, GUILIN CHEN, XUESHUN XIE, YOUXIN ZHOU and ZIWEI DU

Neurosurgery and Brain and Nerve Research Laboratory, The First Affiliated Hospital of Soochow University, Suzhou, Jiangsu 215006, P.R. China

Received December 18, 2014; Accepted September 10, 2015

DOI: 10.3892/mmr.2015.4446

Abstract. In glioma tissues, there are small cell populations with the capability of sustaining tumor formation. These cells are referred to as glioma stem cells (GSCs). However, the presence of subpopulations of GSCs, and the differences between each subpopulation remain to be fully elucidated. In the present study, CD133$^-$/A2B5$^-$ and CD133$^-$/A2B5$^+$ cells from the SHG139 GSC cell line (SHG139s) were isolated using magnetic-activated cell sorting. Following xenografting into nude mice, the two isolated subpopulations generated tumors. The characteristics of the two subpopulations were investigated extensively, and it was found that the two exhibited cancer stem cell characteristics. These cells expressed stem cell markers, exhibited a neurosphere-like appearance, and were found to exhibit self-renewal and multipotency capabilities. Subsequently, the self-renewal and proliferation abilities of the two subpopulations were compared. It was found that the A2B5$^-$ cells had a higher proliferative index and a higher self-renewal ability, compared with the A2B5$^+$ cells. In addition, the A2B5$^-$ cells exhibited increased angiogenic ability. However, the invasion ability of the A2B5$^+$ cells was higher than that of the A2B5$^-$ cells. Taken together, the results of the present study suggested that there are different cell subpopulations in GSCs, and each subpopulation has its own properties.

Introduction

It has been reported that gliomas arise following the malignant transformation of neural stem cells or progenitors (1-4). Glioma stem cells (GSCs) are a rare subpopulation of cells within glioma tissues. GSCs have a distinct self-renewal property and can generate all the heterogeneous lineages of cancer cells, which eventually constitute a tumor (5). GSCs are responsible for the initiation, progression, metastasis and recurrence of cancer (6). Investigations on cancer stem cells (CSCs) may assist in further understanding the mechanisms of development of glioma, and may provide a more effective method for their treatment.

In previous studies, several markers of CSCs have been found, including CD133, SSEA1, CD44 and A2B5 (7-9). However, not all CSCs express all of the above-mentioned stem cell markers. In a previous study, it was reported that only CD133$^+$ cells were found in CSCs (5,10). Subsequent studies by Beier *et al* (5) and Wang *et al* (11) found the existence of CD133$^-$ cells in CSCs. In a previous study, it was reported that A2B5$^+$ cells from glioblastma also exhibit cancer stem-like properties (8). Compared with A2B5$^-$ cells from glioblastoma tissue, A2B5$^+$ cells exhibit more marked tumorigenic potential *in vivo* (7). However, in CSC lines, the differences between A2B5$^-$ and A2B5$^+$ cells remain to be fully elucidated.

In the present study, the differences between A2B5$^-$ cells and A2B5$^+$ cells from the SHG139s GSC line were compared. A SHG139s GCS line possessing the molecular phenotype of CD133^{low}/A2B5^{high} was cultured and developed in a previous study (12). In order to rule out the effect of the expression of CD133, the CD133$^+$ cells were first excluded using magnetic-activated cell sorting (MACS). As A2B5$^-$ and A2B5$^+$ cells from CD133$^-$ SHG139s possess stem cell properties the aim of the present study was to investigate whether expression of A2B5 affects proliferation, invasion, and angiogenesis of CD133$^-$ SHG139s.

Materials and methods

Cell culture. The SHG139s GSC line was developed and provided by the Neurosurgery and Brain and Nerve Research Laboratory, The First Affiliated Hospital of Soochow University, (Suzhou, China). The SHG139s cell line was maintained in stem-cell permissive medium [Dulbecco's modified Eagle's medium (DMEM)-F12 containing 20 ng/ml epidermal growth factor, basic fibroblast growth factor (bFGF; R&D

Correspondence to: Dr Youxin Zhou, Neurosurgery and Brain and Nerve Research Laboratory, The First Affiliated Hospital of Soochow University, 708 Renmin Road, Suzhou, Jiangsu 215006, P.R. China
E-mail: zhouyouxin@suda.edu.cn

*Contributed equally

Key words: glioma stem cells, CD133$^-$, A2B5$^+$, angiogenesis, invasion, SHG139s

Systems, Inc., Minneapolis, MN, USA), nitrogen gas (dilution, 1:50) and B27 (dilution, 1:50; Invitrogen; Thermo Fisher Scientific, Inc., Waltham, MA, USA)].

MACS. The cells were dissociated using 0.25% trypsin (Beyotime Institute of Biotechnology, Haimen, China) and resuspended in phosphate-buffered saline (PBS). All reagents and supplies for MACS separation were purchased from Miltenyi Biotec GmbH (Bergisch-Gladbach, Germany). Selection of $CD133^-$ SHG139s cells was performed, according to the manufacturer's instructions, using CD133/1 Micro Beads. Subsequently, the $CD133^-$ cells were separated from the $A2B5^+$ cells and $A2B5^-$ cells, according to the manufacturer's instructions, using A2B5 Micro Beads.

In vitro invasion assay. The $CD133^-/A2B5^+$ and $CD133^-/A2B5^-$ cells were transferred onto Matrigel-coated invasion chambers (24-well insert, 8-μm pores; BD Biosciences, Franklin Lakes, NJ, USA), containing serum-free DMEM. DMEM containing 10% fetal bovine serum was added to the lower chamber as a chemoattractant. Following an incubation period at 37.5˚C for 48-72 h, non-invading cells were removed from the inner part of the insert using a cotton swab. The cells on the lower membrane surface were fixed in 4% formaldehyde (Beyotime Institute of Biotechnology) and stained with 0.1% crystal violet (Beyotime Institute of Biotechnology). The number of invading cells were manually counted in five randomly-selected fields under a microscope (CKX41SF inverted microscope; Olympus Corporation, Tokyo, Japan) and images were captured.

Western blot analysis. The primary antibodies used in the present study were polyclonal rabbit anti-human tissue inhibitor of metalloproteinase 3 (TIMP3; cat. no. BA0577), polyclonal rabbit anti-human E-cadherin (cat. no. PB0583), polyclonal rabbit anti-human matrix metalloproteinase (MMP) 2 (cat. no. BA0569) and anti-MMP9 (cat. no. BM0573) all purchased from Wuhan Boster Bioengineering Co., Ltd. (Wuhan, China). Total protein from the cells was directly extracted in lysis buffer (Beyotime Institute of Biotechnology) and the concentration of total protein was quantified using an ultraviolet spectrophotometer (Multiskan Mk3; Thermo Fisher Scientific, Waltham, MA, USA). Protein samples (100 or 50 μg) were separated using 12% sodium dodecyl sulfate-polyacrylamide gel electrophoresis (Beyotime Institute of Biotechnology). The proteins were then transferred onto nitrocellulose membranes (Beyotime Institute of Biotechnology) and non-specific binding was blocked by incubating the membranes in 5% non-fat milk. The membranes were incubated at 37˚C with primary antibodies overnight at 4˚C. Following incubation, the membranes were washed with PBS with Tween-20 and incubated at 37˚C for 2 h with horseradish peroxidase (HRP)-conjugated monoclonal goat anti-rabbit secondary antibodies (cat no. Beyotime Institute of Biotechnology; cat. no. A0208), followed by detection and visualization using electrochemiluminescence western blotting detection reagents (Pierce Biotechnology, Inc.; Thermo Fisher Scientific, Inc.). Quantification of protein expression was performed by measuring the gray-scale value of bands using ImageJ software (version 2.1.4.7; National Institutes of Health, Bethesda, MD, USA).

Subcutaneous implanted models. A total of 16 nude mice were separated into two groups (each group comprised of four female and four male mice). The mice were aged ~4-6 weeks and weighed 24-28g. The mice were raised in specific-pathogen free conditions, and the temperature was maintained between 26 and 28˚C. The mice were exposed to ~10 h light per day, and given food and water following high-temperature sterilization. The mice were raised separately, but under the same conditions and were fed standard chow. To investigate the effects of A2B5 expression on tumor growth *in vivo*, cells ($1x10^6$) from the two groups ($CD133^-/A2B5^+$ and $CD133^-/A2B5^-$) were injected into the left axilla of nude mice (n=8). For the injection, the cells were suspended in DMEM-F12 to the same concentration ($1x10^7$ cells/ml) and 100 μl cell suspension was injected into each of the mice on the same day. On day 17 post-implantation, caliper measurements were performed to assess tumor growth.

Immunohistochemistry (IHC) and immunofluorescence (ICC). Mice received an intraperitoneal injection of 45 mg/kg pentobarbital sodium (Shanghai Westang Bio-tech Co., Ltd., Shanghai, China) for anesthetization. The tumors (weight, 1-2.5 g) were excised using tweezers and scissors, and the mice were sacrificed by cervical dislocation. The formalin-fixed paraffin-embedded (Qilin Environmental Technology Firm, Guangzhou, China) SHG139s tumors were cut into 6-μm sections using a microtome (RM2016; Leica Biosystems, Nussloch, Germany). Antigen retrieval was performed in 10 mM sodium citrate buffer (pH 6; Beyotime Institute of Biotechnology) for 16 min at 96-98˚C. The slides were then incubated with primary antibodies against MMP9, MMP2, E-cadherin, TIMP3 and Ki-67 (cat. no. BA2888; Wuhan Boster Bioengineering Co., Ltd.), and with antibodies against vascular endothelial growth factor (VEGF; cat. no. ab46154), VEGF receptor 2 (VEGFR2; cat. no. ab2349) and CD34 (cat. no. ab81289; Abcam, Tokyo, Japan). The sections were subsequently incubated with a cell and tissue HRP-DAB staining system (R&D Systems, Inc., Minneapolis, MN, USA), according to the manufacturer's instructions. Immunostaining was performed using tumor controls that were positive (tumors formed by $A2B5^+$ cells) and negative (tumors formed by $A2B5^-$ cells), and was evaluated by a pathologist in a blinded-manner. For ICC staining, the cells were seeded onto coverslips (~$5x10^5$ cells/ml) and fixed with 4% paraformaldehyde (Sigma-Aldrich), treated with 3% hydrogen peroxide for 10 min and incubated with the antibodies, described above, overnight at 4˚C. Fluorescein isothiocyanate- or tetramethylrhodamine isothiocyanate-labeled goat anti-rabbit secondary antibodies (1:200; cat. no. ab97178; Abcam) were then added and incubated for 2 h at 37˚C. The 4',6-diamidino-2-phenylindole reagent (Wuhan Boster Bioengineering Co., Ltd.) was used to stain the cell nuclei, and the cells were visualized using fluorescence microscopy (BX40F4; Olympus Corporation).

Secondary sphere forming assay. The cells, which were isolated using MACS were seeded (100 cells/well) into 96-well plates in the presence of the stem cell-permissive medium (0.2 ml). The cultures were maintained by replacing half of the medium every 3 days. A subsphere-forming assay (also termed passaging) was repeated every 2 weeks. Following each passage, the number and the size of the spheres were

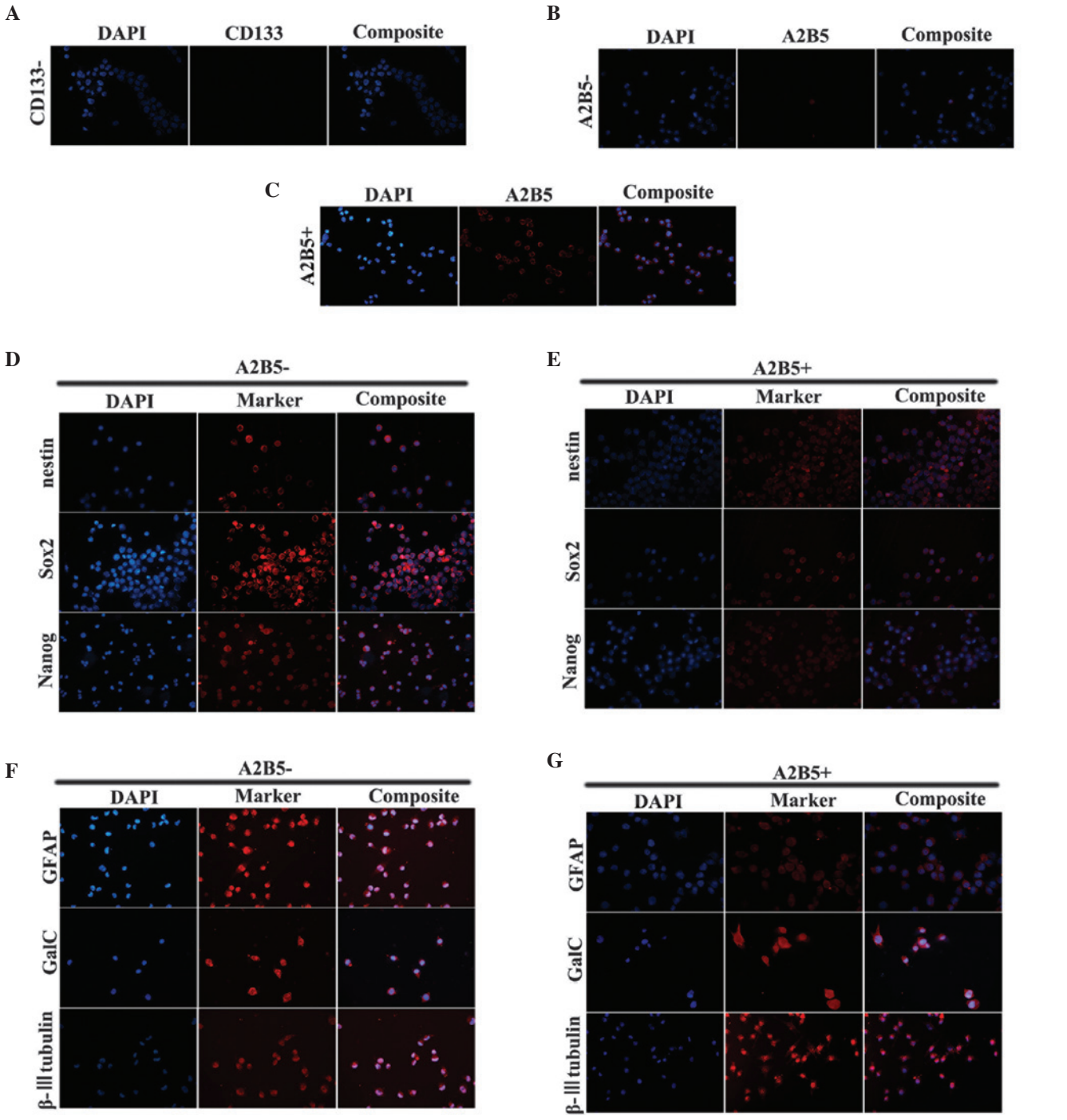

Figure 1. ICC analysis revealing the purity of $CD133^-/A2B5^-$ and $CD133^-/A2B5^+$ cells from SHG139s by MACS. Stem cell markers of each subpopulation are shown, with the multiple differentiation potential of $A2B5^-$ and $A2B5^+$ cells in serum-containing medium (magnification, x400). (A) ICC analysis showing the purity of $CD133^-$ cells from the SHG139s using MACS. (B) ICC analysis showing the purity of $A2B5^-$ cells from $CD133^-$ SHG139s using MACS. (C) ICC analysis showing the purity of $A2B5^+$ cells from $CD133^-$ SHG139s. (D and E) ICC analysis showing the expression of stem cell markers of $CD133^-/A2B5^-$ and $CD133^-/A2B5^+$ cells. (F and G) ICC analysis showing the differentiation markers of the differentiated cells from $A2B5^-$ and $A2B5^+$ cells. ICC, immunofluorescence; MACS, magnetic-activated cell sorting; Sox2, sex determining region Y-box 2; Galc, galactosylceramidase; GFAP, glial fibrillary acidic protein.

assessed, on days 7 and 14, under a CKX41SF inverted microscope.

Cell cycle analysis and cell proliferation assay. Cells were collected in an exponential growth phase and then fixed with ethanol. Subsequently, RNase A treatment (Beyotime Institute of Biotechnology) and propidium iodide staining were performed. The cells were detected using flow cytometry with a FACSCalibur (BD Biosciences). The number of cells at the G_0/G_1, S and G_2/M phases were quantified using Modfit software (BD Biosciences), excluding the calculation of cell debris and fixation artifacts. Cell proliferation was quantified using a Cell Counting Kit-8 (CCK-8; Beyotime Institute of Biotechnology). Briefly, 100 μl cells (suspended in stem-cell permissive medium) from the two groups ($CD133^-/A2B5^+$and $CD133^-/A2B5^+$ cells) were seeded onto a 96-well plate at a

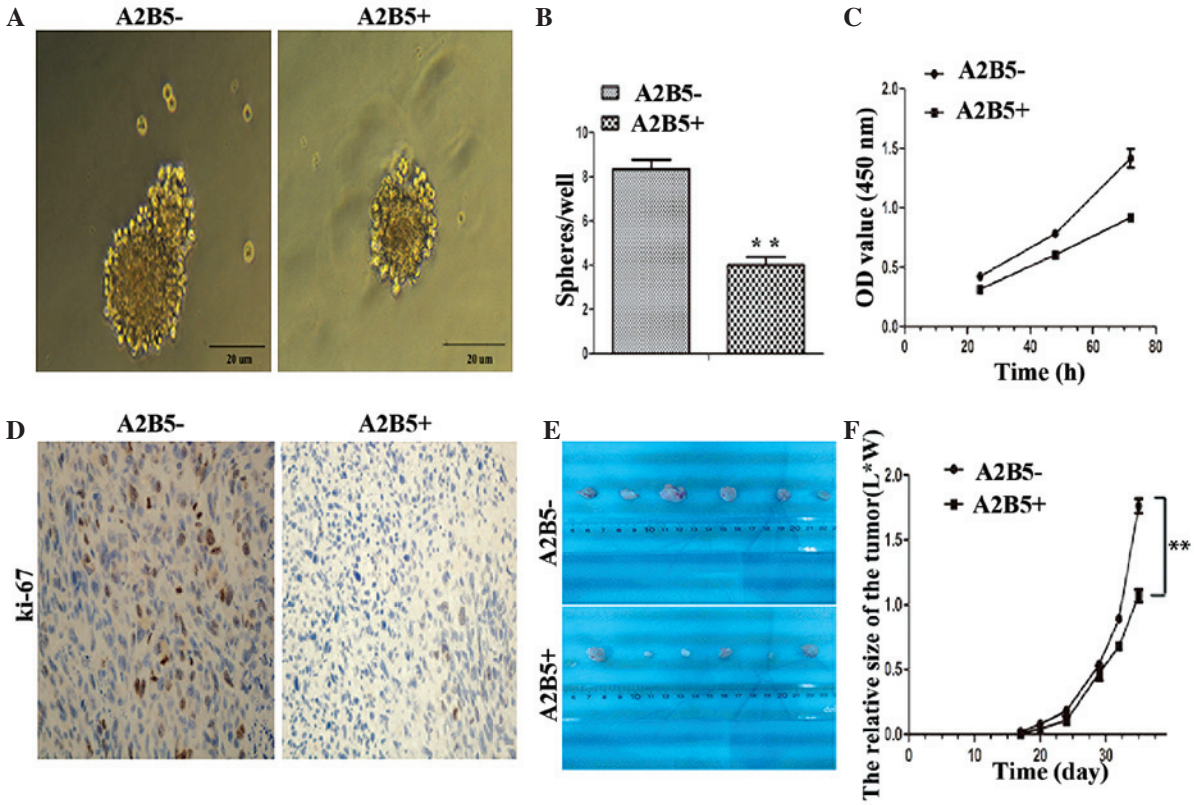

Figure 2. Self-renewal and proliferation abilities of the A2B5$^-$ and A2B5$^+$ subpopulations. (A and B) Secondary sphere forming assay revealed that the expression of A2B5 affected the size and number of spheres (magnification, x100). (C) Cell counting Kit-8 assays revealed that the proliferation ability of the A2B5$^-$ cells was higher than that of the A2B5$^+$ cells. (D) Immunohistochemical analysis revealed that the expression of A2B5 reduced the expression of Ki-67 in the nude subcutaneous glioma mouse model (magnification, x400). (E and F) Expression levels of A2B5 reduced glioma growth in a subcutaneous glioma nude mouse model (**P<0.05). Data are expressed as the mean ± standard error. OD, optical density.

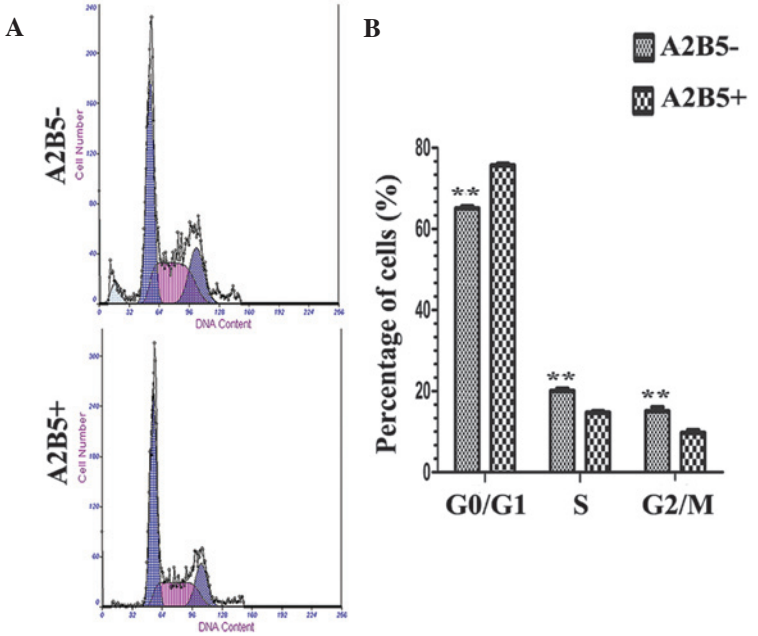

Figure 3. Flow cytometric analysis of the cell cycle of the A2B5$^-$ and A2B5$^+$ cells (**P<0.05). (A) Flow cytometry and (B) quantification of the percentages of cells in each phase of the cell cycle. Data are expressed as the mean ± standard error.

concentration of 2,000/cells per well and incubated at 37˚C. At daily intervals (1, 2 and 3 days), the optical density was measured at 450 nm using a microtiter plate reader (Thermo Multiskan MK3; Thermo Fisher Scientific, Inc.) with the cell survival rate expressed as the absorbance. The results represent the average of six replicates under the same conditions.

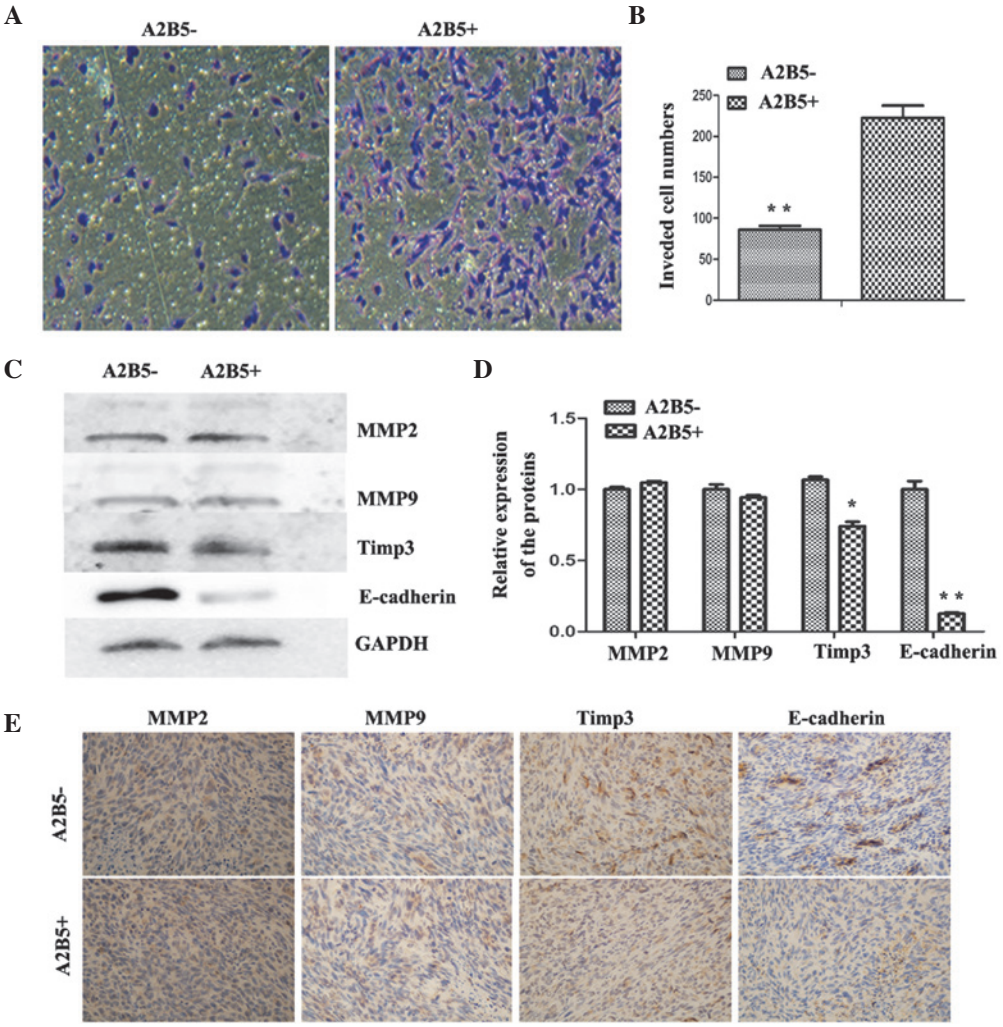

Figure 4. Expression of A2B5 promotes the invasion of cells *in vivo* and *in vitro*. (A and B) Analysis using a Transwell invasion system showed that the numbers of invasive cells were significantly reduced in the A2B5$^-$ cells, compared with the A2B5$^+$ cells (magnification, x100). Data are expressed as the mean ± standard deviation of three independent experiments (P<0.01). (C and D) Western blot analysis showed that the expression of A2B5 led to downregulation in the expression levels of TIMP3 and E-cadherin. Data are expressed as the mean ± standard deviation of three independent experiments (*P<0.05 and **P<0.01, vs. A2B5$^-$). (E) Immunohistochemical analysis showed that the expression of A2B5 reduced the expression levels of TIMP3 and E-cadherin (magnification, x400). Data are expressed as the mean ± standard error. MMP, matrix metalloproteinase; TIMP3, tissue inhibitor of metalloproteinase 3.

Statistical analysis. Statistical analyses were performed using SPSS software, version 13.0 (SPSS, Inc., Chicago, IL, USA). Statistical significance was determined using two-tailed Student's t-test and data are expressed as the mean ± standard error. P<0.05 was considered to indicate a statistically significant difference.

Results

Isolation and stem cell characteristics of CD133$^-$/A2B5$^+$ and CD133$^-$/A2B5$^-$ cells of SHG139s. The SHG139s cells were dissociated using 0.25% trypsin, following which the cells were subjected to MACS. The results revealed two groups of cells: CD133$^-$/A2B5$^+$ and CD133$^-$/A2B5$^-$ cells. The purity of the isolated cells was determined using ICC, and the purity of the two groups was >90% (Fig. 1A-C).

The ICC staining also demonstrated that the majority of cells in the two subpopulations expressed Nestin, sex determining region Y-box 2 (Sox2) and Nanog stem cell markers (Fig. 1D and E). To assess the differentiation potential of the cells, the two populations of cells were cultured in serum-containing medium. The cells presented with adherent growth. The expression levels of glial fibrillary acidic protein (GFAP), β-III tubulin and galactosylceramidase (Galc) were assessed using ICC. The adherent cells in the two groups exhibited expression of the three differentiation markers (Fig. 1F and G).

Self-renewal and proliferation ability of CD133$^-$/A2B5$^-$-derived cells. An *in vitro* sphere formation assay was used to examine whether the expression of A2B5 was involved in cell renewal upon serial passaging. It was found that the high expression level of A2B5 not only affected the size of the spheres, but also led to the reduction in the numbers of spheres in subsequent generations (Fig. 2A and B). To investigate whether the expression of A2B5 affected the proliferation of cells *in vitro*, a CCK-8 assay (Fig. 2C) and flow cytometric analysis of the cell cycle were performed. The results showed that the proliferation abilities of the A2B5$^-$-derived cells were more marked than those of the A2B5$^+$-derived cells. Furthermore, to probe the effects of high expression levels of A2B5 on cancer cell growth *in vivo*, a

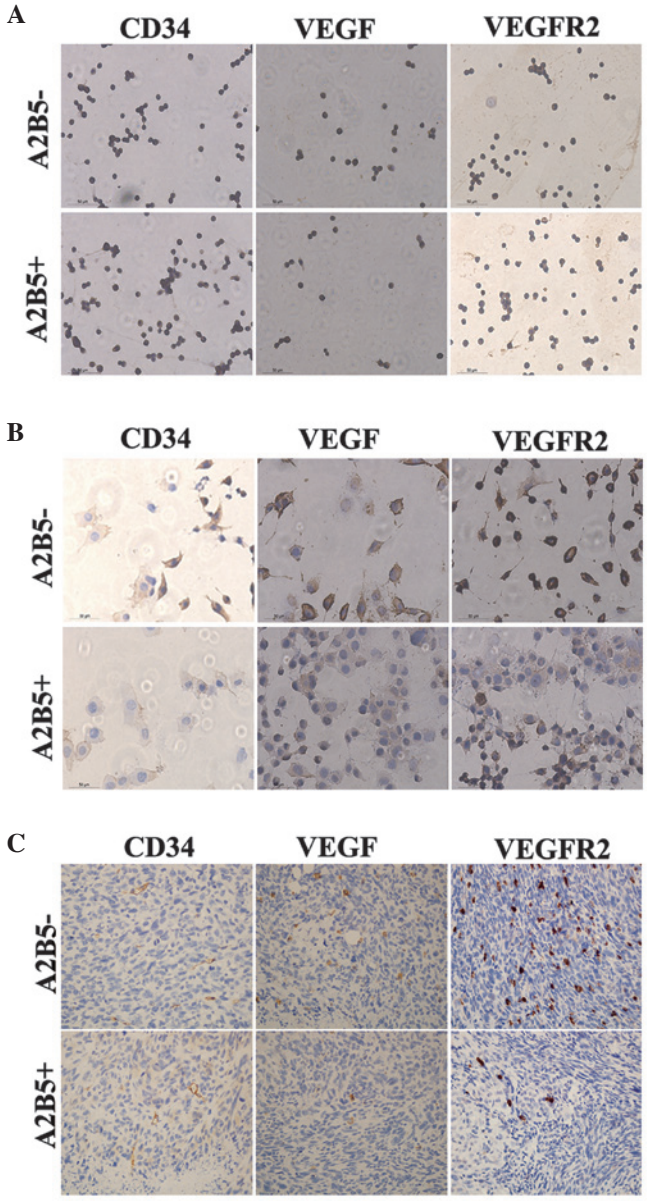

Figure 5. Expression of A2B5 promotes the expression of markers associated with angiogenesis *in vitro* and *in vivo*. (A) IHC analysis revealed high expression levels of CD34, VEGF and VEGFR2 in the A2B5$^-$ and A2B5$^+$ cells from SHG139s. (B) IHC analysis revealed higher expression levels of VEGF and VEGFR2 in the cells differentiated from A2B5$^-$ cells. (C) IHC revealed that the expression of A2B5 promoted the expression levels of VEGF and VEGFR2 *in vivo*. (Magnification, x400). IHC, immunohistochemical; VEGF, vascular endothelial growth factor; VEGFR2, VEGF receptor 2.

mouse model of human glioma was used. The A2B5$^-$-derived cells and A2B5$^+$-derived cells were injected into the left axilla of nude mice. The results showed that the two A2B5 subtypes had similar tumorigenicity in nude mice *in vivo*. However, that the expression levels of Ki-67 in the tumors formed from the A2B5$^-$-derived cells were higher, compared with those formed by the A2B5$^+$-derived cells (Fig. 2D). In addition, the growth of the tumors from the A2B5$^+$-derived cells was significantly inhibited, compared with that of the tumors formed by the A2B5$^-$-derived cells (Fig. 2E and F; P<0.05).

Effect of A2B5 on cell cycle. The results of flow cytometry indicate that A2B5 expression increased the percentage of G_0/G_1 phase cells, and decreased the percentage of S and G_2/M phase cells (P<0.05; Fig. 3).

Comparison of the invasion abilities of the A2B5$^-$- and A2B5$^+$-derived cells. To assess the effects of high expression levels of A2B5 on the invasiveness of glioma cells, a Transwell invasion system was used. The number of invasive cells from the A2B5$^-$-derived cells was significantly reduced, compared with the A2B5$^+$-derived cells (Fig. 4A and B). To further examine the molecular associations between the high expression levels of A2B5 and invasiveness in human glioma, the relative expression levels of MMP9, MMP2, E-cadherin and TIMP3 were analyzed using western blot analysis. The results revealed no difference in the expression levels of MMP2 and MMP9, whereas E-cadherin and TIMP3 were expressed at high levels in the A2B5$^-$-derived cells (Fig. 4C and D). The subcutaneous tumors were removed and sectioned, and the sections were stained with antibodies against MMP2, MMP9, E-cadherin and TIMP3. Subsequent IHC analysis showed that the tumors formed from A2B5$^-$-derived cells had higher expression levels of E-cadherin and TIMP3; however, no difference was observed between the expression levels of MMP2 and MMP9 (Fig. 4E). Thus, the data indicated that higher expression levels of A2B5 led to enhancement of glioma cell invasion in the tumor xenografts.

Angiogenesis of the two cell subpopulations. To assess the angiogenesis of the two groups of cells, the expression levels of CD34, VEGF and VEGFR2 in the differentiated cells of each group were assayed using IHC (13-15). No significant difference was observed between the percentages of CD34-positive cells between the two groups (Fig. 5A). However, the percentage of VEGF-positive and VEGFR2-positive cells in the differentiated cells from the A2B5$^-$-derived cells were higher than those in the A2B5$^+$-derived cells (Fig. 5B). In addition, these three indicators were assessed *in vivo* using IHC. A small number of CD34$^+$ cells were involved in the formation of tumors in the two groups. Tumors formed by A2B5$^-$-derived cells exhibited higher expression levels of VEGF and VEGFR2 (Fig. 5C).

Discussion

CD133 is a 5-transmembrane glycoprotein, expressed in the membranes of human hematopoietic cells and neural progenitor cells. Singh *et al* (10) demonstrated that 100 CD133$^+$ cells from glioblastoma multiforme (GBM) were able to form a tumor in mice, which was similar to the original patient tumor, suggesting that CD133$^+$ cells from GBM exhibit GSC properties (16). However, Beier *et al* reported the existence of CD133$^-$ GSCs in a later study (5). The results of the present stud also confirmed the existence of CD133$^-$ GSCs.

A2B5 is a type of multi monosialoganglioside, which is expressed on the cell surface. It is also a marker of progenitors of oligodendrocyte-type-2-astrocyte (O-2A). Tchoghandjian *et al* (7) reported that A2B5$^+$ cells isolated from GBM can form spheres. Previous flow cytometric characterization of A2B5$^+$-derived spheres revealed three distinct populations of cells: A2B5$^+$/CD133$^+$, A2B5$^+$/CD133$^-$ and A2B5$^-$/CD133$^-$ cells (7). CD133$^+$/A2B5$^+$ and CD133$^-$/A2B5$^+$ cells exhibit CSC properties, and it has been shown that

$A2B5^+$ cells are crucial for the initiation and maintenance of GBM, whereas the expression of CD133 is more involved in determining tumor behavior (7). Ogden *et al* (13) reported that the majority of gliomas can be divided into the three subpopulations described above; and it has been demonstrated that the tumorigenic potential of the $CD133^+/A2B5^+$ and $CD133^-/A2B5^+$ cells are more marked, compared with that of the $CD133^-/A2B5^-$ cells. Similarly, in the present study, three distinct populations of cells from SHG139 lines were isolated using MACS. The cell purity of the isolated cells populations was determined using ICC and flow cytometry, which revealed all three cells subpopulations had >90% purity. In a previous study, it was found that $CD133^-/A2B5^+$ and $CD133^-/A2B5^-$ cells can form tumors in mice, and have similar tumorigenic potential. Therefore, the present study focussed predominantly on comparing the other functions of $CD133^-/A2B5^+$ and $CD133^-/A2B5^-$ cells. It was found that the groups of the cells exhibited characteristics of CSCs, and confirmed the existence of $CD133^-/A2B5^-$GSCs in the SHG139s cells, whereas a previous study reported that only $A2B5^+/CD133^+$ and $A2B5^+/CD133^-$ cells from $A2B5^+$-derived cells exhibit CSC characteristics (7,13). This contradictory result may be caused by the differences between different GSC lines. Tchoghandjian *et al* (7) isolated the GSCs of $A2B5^+$ cells derived from GBM; however, it was not clear whether there were $A2B5^-$ GSCs in the GBM, which requires ruling out to confirm that the GSC characteristics are part of the $A2B5^+$ cells. In the present study, the SHG139s cells were derived from SHG139 glioma cells by culturing SHG139 in stem cell-permissive medium. In the previous study, it was demonstrated that SHG44 GSCs (SHG44s) were $CD133^{high}/A2B5^{low}$, which indicated that not all GSCs express A2B5 at high levels (16). Notably the present study confirmed the existence of $A2B5^-$GSCs.

In the present study, the results of the Tanswell assay showed that the number of invasive $A2B5^+$ cells was increased, compared with the $A2B5^-$ cells. Subsequently, indicators, including MMP2, MMP9, E-cadherin and TIMP3, that are associated with invasion, were examined using western blot and IHC analyses (17-20). The results showed no difference in the expression levels of MMP2 and MMP9; however, the expression levels of E-cadherin and TIMP3 in the $A2B5^+$-derived cells were reduced, compared with the $A2B5^-$-derived cells. This indicated that the $A2B5^+$-derived cells promoted invasion by reducing the expression levels of E-cadherin and TIMP3. The assays comparing the ability of self-renewal and proliferation showed that the self-renewal and proliferation abilities of the $A2B5^-$-derived cells were more marked, compared with the $A2B5^+$-derived cells. Usually, if a gene promotes invasion, it will also promote proliferation (7,21,22). However, the results of the present study are contradictory to this, which may be due to the inherent properties of GSCs. Accordingly, different subpopulations may exist in the GSCs, with certain cell subpopulations responsible for proliferation and other subpopulations responsible for invasion.

In the present study, the expression levels of CD34, VEGF and VEGFR2 in the GSCs and their differentiated cells were examined using IHC analysis. The results showed that VEGF and VEGFR2 were expressed at high levels in the GSCs, indicating that high expression levels of VEGF and VEGFR2 are characteristic of GSCs. However, the expression levels of VEGF and VEGFR2 in the cells differentiated from $A2B5^-$ cells were higher than those in the cells differentiated from $A2B5^+$ cells. The IHC analysis of *in vivo* tumor tissues also revealed the same results, indicating that $A2B5^-$-derived cells had increased angiogenic ability. In a previous study, specific anti-human CD34 IHC analysis of tumor samples revealed that a small number of $CD34^+$ cells were involved in tumor formation and may also be involved in the formation of vascular mimicry (23).

In conclusion, the results of the present study revealed the effects of the expression of A2B5 on the phenomenon of GSCs. Future investigations are likely to further elucidate the regulatory mechanisms of A2B5 on GSCs, and may provide a novel therapeutic approach to eliminate GSCs.

Acknowledgements

The authors would like to thank the Animal Research Institute of Nanjing University for providing the nude mice. This study was supported by the National Natural Science Foundation of China (grant. no. 81372689), the Major Issues Foundation of the Health Department of Jiangsu Province (grant. no. K201106) and the Six Big Talent Peak Project in Jiangsu province. (grant. no. 2012-WS-050).

References

1. Galli R, Binda E, Orfanelli U, Cipelletti B, Gritti A, De Vitis S, Fiocco R, Foroni C, Dimeco F and Vescovi A: Isolation and characterization of tumorigenic, stem-like neural precursors from human glioblastoma. Cancer Res 64: 7011-7021, 2004.
2. Hemmati HD, Nakano I, Lazareff JA, Masterman-Smith M, Geschwind DH, Bronner-Fraser M and Kornblum HI: Cancerous stem cells can arise from pediatric brain tumors. Proc Natl Acad Sci USA 100: 15178-15183, 2003.
3. Ignatova TN, Kukekov VG, Laywell ED, Suslov ON, Vrionis FD and Steindler DA: Human cortical glial tumors contain neural stem-like cells expressing astroglial and neuronal markers in vitro. Glia 39: 193-206, 2002.
4. Singh SK, Clarke ID, Terasaki M, Bonn VE, Hawkins C, Squire J and Dirks PB: Identification of a cancer stem cell in human brain tumors. Cancer Res 63: 5821-5828, 2003.
5. Beier D, Hau P, Proescholdt M, Lohmeier A, Wischhusen J, Oefner PJ, Aigner L, Brawanski A, Bogdahn U and Beier CP: CD133(+) and CD133 (-) glioblastoma-derived cancer stem cells show differential growth characteristics and molecular profiles. Cancer Res 67: 4010-4015, 2007.
6. Zhou C and Sun B: The prognostic role of the cancer stem cell marker aldehyde dehydrogenase 1 in head and neck squamous cell carcinomas: A meta-analysis. Oral Oncol 50: 1144-1148, 2014.
7. Tchoghandjian A, Baeza N, Colin C, Cayre M, Metellus P, Beclin C, Ouafik L and Figarella-Branger D: A2B5 cells from human glioblastoma have cancer stem cell properties. Brain Pathol 20: 211-221, 2010.
8. Son MJ, Woolard K, Nam DH, Lee J and Fine HA: SSEA-1 is an enrichment marker for tumor-initiating cells in human glioblastoma. Cell Stem Cell 4: 440-452, 2009.
9. Lathia JD, Gallagher J, Heddleston JM, Wang J, Eyler CE, Macswords J, Wu Q, Vasanji A, McLendon RE, Hjelmeland AB and Rich JN: Integrin alpha 6 regulates glioblastoma stem cells. Cell Stem Cell 6: 421-432, 2010.
10. Singh SK, Hawkins C, Clarke ID, Squire JA, Bayani J, Hide T, Henkelman RM, Cusimano MD and Dirks PB: Identification of human brain tumour initiating cells. Nature 432: 396-401, 2004.
11. Wang J, Sakariassen PØ, Tsinkalovsky O, Immervoll H, Bøe SO, Svendsen A, Prestegarden L, Røsland G, Thorsen F and Stuhr L: CD133 negative glioma cells form tumors in nude rats and give rise to CD133 positive cells. Int J Cancer 122: 761-768, 2008.

12. Chen GL, Li YY, Xie XS, Chen JM, Wu TF and Li XT: The establishment of a new human glioma cell line and its biological characteristic analysis. Chin J Oncol 39: 1-7, 2014.
13. Ogden AT, Waziri AE, Lochhead RA, Fusco D, Lopez K, Ellis JA, Kang J, Assanah M, McKhann GM, Sisti MB, *et al*: Identification of A2B5+CD133- tumor-initiating cells in adult human gliomas. Neurosurgery 62: 505-514; discussion 514-515, 2008.
14. Kumagai Y, Sobajima J, Higashi M, Ishiguro T, Fukuchi M, Ishibashi K, Baba H, Mochiki E, Yakabi K, Kawano T, *et al*: Angiogenesis in superficial esophageal squamous cell carcinoma: Assessment of microvessel density based on immunostaining for CD34 and CD105. Jpn J Clin Oncol 44: 526-533, 2014.
15. Takahashi H, Inoue A, Kawabe Y, Hosokawa Y, Iwata S, Sugimoto K, Yano H, Yamashita D, Harada H, Kohno S, *et al*: Oct-3/4 promotes tumor angiogenesis through VEGF production in glioblastoma. Brain Tumor Pathol 32: 31-40, 2015.
16. Wu TF, Chen JM, Chen SS, Chen GL, Wei YX, Xie XS, Du ZW and Zhou YX: Phenotype of SHG-44 glioma stem cell spheres and pathological characteristics of their xenograft tumors. Zhonghua Zhong Liu Za Zhi 35: 726-731, 2013 (In Chinese).
17. Yang X, Du WW, Li H, Liu F, Khorshidi A, Rutnam ZJ and Yang BB: Both mature miR-17-5p and passenger strand miR-17-3p target TIMP3 and induce prostate tumor growth and invasion. Nucleic Acids Res 41: 9688-9704, 2013.
18. Li H, Chen X, Gao Y, Wu J, Zeng F and Song F: XBP1 induces snail expression to promote epithelial- to-mesenchymal transition and invasion of breast cancer cells. Cell Signal 27: 82-89, 2015.
19. Huang D, Du X, Yuan R, Chen L, Liu T, Wen C, Huang M, Li M, Hao L and Shao J: Rock2 promotes the invasion and metastasis of hepatocellular carcinoma by modifying MMP2 ubiquitination and degradation. Biochem Biophys Res Commun 453: 49-56, 2014.
20. Jia LF, Wei SB, Mitchelson K, Gao Y, Zheng YF, Meng Z, Gan YH and Yu GY: miR-34a Inhibits migration and invasion of tongue squamous cell carcinoma via targeting MMP9 and MMP14. PloS one 9: e108435, 2014.
21. Tan J, Yang S, Shen P, Sun H, Xiao J, Wang Y, Wu B, Ji F, Yan J, Xue H and Zhou D: C-kit signaling promotes proliferation and invasion of colorectal mucinous adenocarcinoma in a murine model. Oncotarget: Sep 2, 2015 (Epub ahead of print).
22. Zhuo Z, Yang XF, Huang KQ, Ren L, Zhao S, Gou WF, Shen DF, Sun HZ, Takano Y and Zheng HC: The upregulated α-catulin expression was involved in head-neck squamous cell carcinogenesis by promoting proliferation, migration, invasion, and epithelial to mesenchymal transition. Tumour Biol: Aug 27, 2015 (Epub ahead of print).
23. Liu TJ, Sun BC, Zhao XL, Zhao XM, Sun T, Gu Q, Yao Z, Dong XY, Zhao N and Liu N: CD133+ cells with cancer stem cell characteristics associates with vasculogenic mimicry in triple-negative breast cancer. Oncogene 32: 544-553, 2013.